Supporting information

A Facile Method to Synthesize Pt-Ni Octahedral Nanoparticles with Porous and Open-Structure Features for Enhanced Oxygen Reduction Catalysis

Zheng Jiang, Yang Liu, Lei Huang, Wen Hao Gong and Pei Kang Shen*

Collaborative Innovation Center of Renewable Energy Materials, Guangxi Key Laboratory of Electrochemical Energy Materials, College of Chemistry and Chemical Engineering, State Key Laboratory of Processing for Non-Ferrous Metal and Featured Materials, Guangxi University, Nanning 530004, P. R. China

Number of pages: 16
Number of tables: 1
Number of figures: 12

Table of Contents

Experimental Details:

Chemicals: Chloroplatinic acid hexahydrate ($H_2PtCl_6 \cdot 6H_2O$), nickel acetylacetonate ($Ni(acac)_2$, 95%), N, N-dimethylformamide (DMF, 99.9%), cetyltrimethyl ammonium chloride (CTAC, 97%), acetic acid (95%) and polyvinylpyrrolidone K30 (PVP) were purchased from Aladdin. All chemicals were used as received without further purification. The water used in all experiments was ultrapure (18.2 MΩ). Solvents such as ethanol and hexane were analytical grade and used as received without further purification.

Synthesis of co-deposition Pt-Ni nanoparticle (CON): 160 mg CTAC, 100mg PVP and 35mg $Ni(acac)_2$ were added into the 25mL Teflon-lined autoclave containing 10 mL DMF, Mixed solution in the autoclave was stirred for 10 min at 25 °C, then 13.3mg $H_2PtCl_6 \cdot 6H_2O$ was added. The autoclave was sealed in a stainless steel and transferred into an oil bath with the temperature holding at 160 °C and moderate magnetic stirring. After 12h, autoclave was cooled down to room temperature naturally. The products were collected using alcohol via centrifugation (5000rpm for 5 min).

Synthesis of porous octahedral Pt-Ni nanoparticle (PON): The PON was made from a CON by etching the Ni component by acetic acid. The as-obtained CON was dispersed into 10 mL acetic acid. After sonication (100 W) for 3h at 80 °C, the product was collected by centrifugation, washed with ethanol and dispersed in hexane for further use.

Synthesis of tiny octahedral Pt-Ni nanoparticle (TON): 150 mg CTAC, 80mg PVP and 7mg $Ni(acac)_2$ were added into the 25mL Teflon-lined autoclave containing 10 mL

DMF, the mixed solution in the autoclave was stirred for 10 min at 25°C, then 13.3mg $H_2PtCl_6 \cdot 6H_2O$ was added. The autoclave was sealed in a stainless steel and transferred into an oil bath with the temperature holding at 160 °C and moderate magnetic stirring. After 8h, autoclave was cooled down to room temperature naturally. The products were collected using alcohol via centrifugation (5000rpm for 5 min).

Materials Characterizations: The X-ray diffraction (XRD) measurements were collected on a SmartLab 3 X-ray diffractometer (Rigaku, Japan), with Cu Kα radiation (λ = 1.5405 Å) at 40 KV and 30mA. The 2θ angular regions were from 10° to 90° which were finely scanned at 5° min^{-1}. TEM images were performed on TITAN G2 (FEI, American) microscope at 120 KV. High resolution-TEM, high angle annular dark field scanning transmission electron microscope (HAADF-STEM) and EDS mapping images were performed using TITAN G2 60-300 equipped with image corrector and highly sensitive Super-X energy dispersive X-ray (EDS) detector system. The samples for TEM characterizations were prepared by droping ethyl alcohol disperson of nanocrystals onto caebon-coated Cu grids and immediately evaporatiing the solvent. The concentration of catalysts was determined by the inductively coupled plasma atomic emission spectroscopy (TJA RADIAL IRIS 1000 ICP-AES, USA).

Electrochemical study: The as-obtained Pt-Ni nanoparticles were dispersed on the commercial carbon support (Cabot, Vulcant-72). The organic surfactants were removed by n-butylamine and annealing in air at 200 °C for 1h. The commercial Pt/C catalyst (TKK, Japan) was used for comparison. The catalyst ink was prepared by mixing carbon supported catalysts in 2 mL of solution containing 1.8 mL of ethanol and 200

μL of 0.5 wt. % Nafion solution followed by untrasonication for 30 min. A certain amount of catalyst suspension was pipetted onto the clean glassy carbon surface with a micropipette and dried to form a uniform thin film which was further characterized in electrochemical cell. The Pt loadings for electrocatalysts were normalized over the geometric electrode area of 0.196 cm^2 and determined by ICP-AES. The Pt loadings were 10.7 μg cm^{-2}, 14.28 μg cm^{-2} and 17.8 μg cm^{-2} for PON, TON and TKK-Pt/C respectively.

The electrochemical measurements were conducted in a three-compartment electrochemical cell with a Pine rotational ring-disk electrode (RRDE) setup connected with a biopotentiostat (AFCBP1E, Pine Instrument Co., USA), glassy carbon covered with thin catalyst film acts as a working electrode, reversible hydrogen electrode (RHE) as a reference electrode and Pt flag as a counter electrode. The CV curves were recorded in N_2-saturated 0.1 M $HClO_4$ solution with scan rate of 50 mV s^{-1}. The ORR polarization curves were collected in O_2-saturated 0.1 M $HClO_4$ solution at 1600 rpm with a scan rate of 10 mV s^{-1}. The accelerated durability tests (ADTs) were performed in O_2-saturated 0.1 M $HClO_4$ solutions by applying cyclic potential sweeps between 0.6 and 1.0 V versus RHE at a sweep rate of 100 mV s^{-1} for 6,000 cycles.

Computational Details. DFT calculations were performed on the Dmol[3] program package. The exchanged and correlated interaction were presented by Generalized gradient approximation (GGA) with Perdew-Burlce-Ernzerhof (PBE) function. Spin-polarized was unrestricted for all calculations. Double numerical plus polarization (DNP) basis set was employed and its accuracies equaled to Pope's 6-31G** basis set.

Three calculated models were the octahedron consisting of 114 Ni atoms and 1 Pt atom (at vertex, edge and surface). The total energy of the three octahedrons and The PDOS of Pt 5d electrons were calculated respectively. The k-point sampling of Brillouin zone was obtained with a 3×3×3 grid mesh using Monkhorst-Pack method. The convergence criterion of energy lower than 10 Ha, 0.002 Ha/Å of maximum force, and 0.005 Å of maximum displacement were used for all structure geometry optimization.

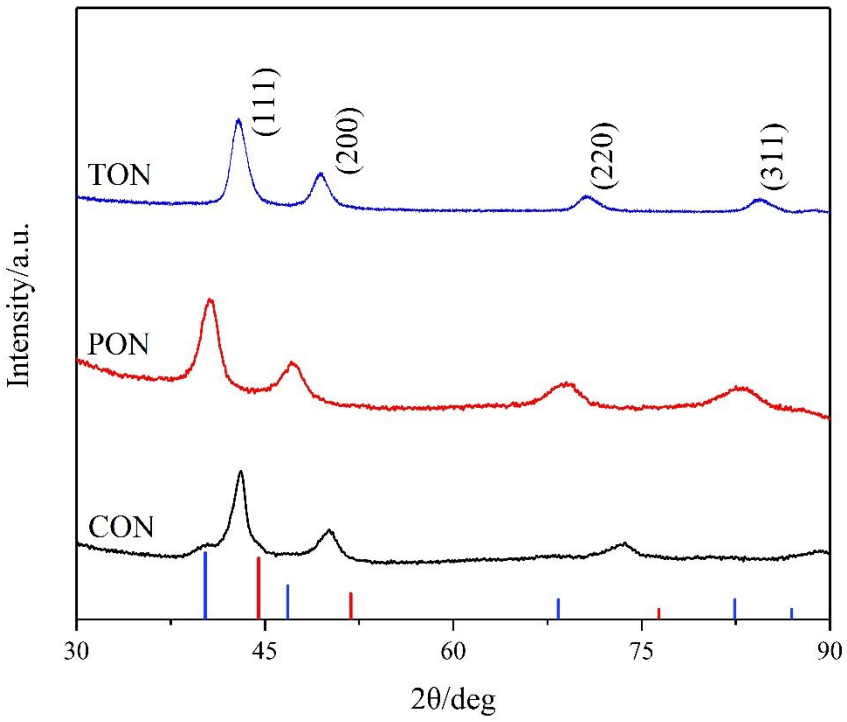

Figure S1: XRD patterns of CON, PON and TON. Color sticks indicate the reference X-ray diffraction lines: blue, Pt (PDF#87-0647), and red, Ni (PDF#87-0712).

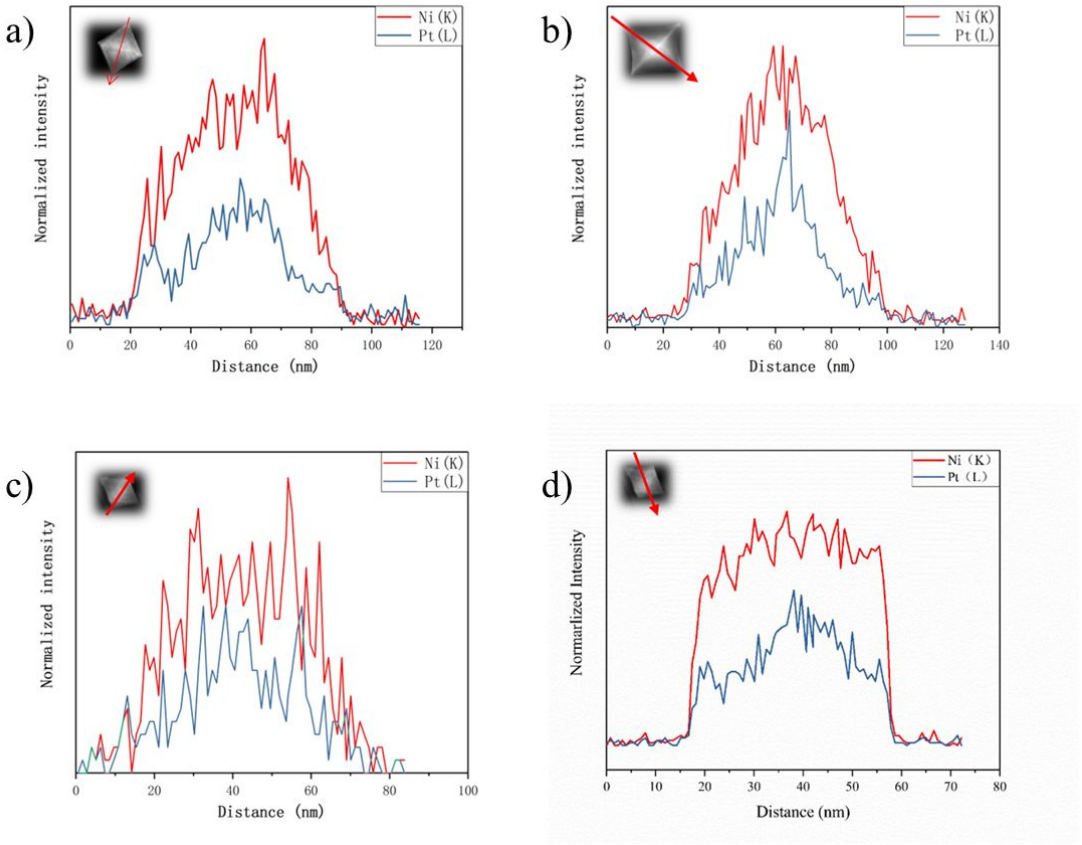

Figure S2: The line scanning image of CON for four different scanning directions.

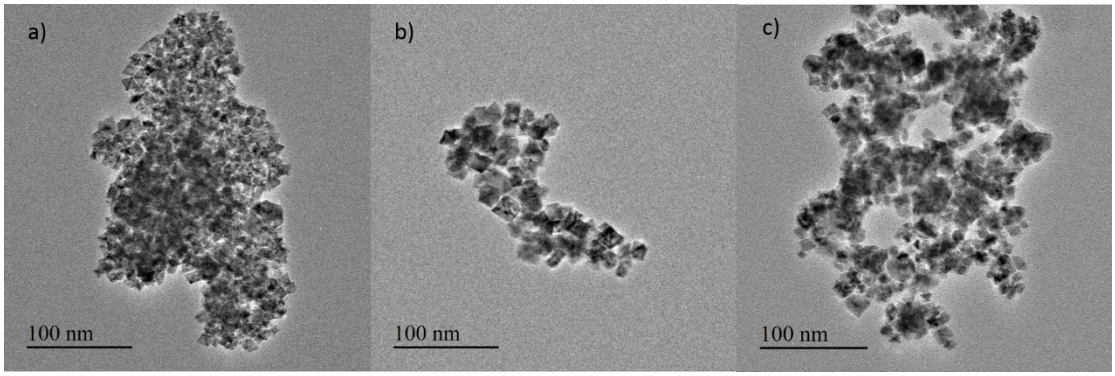

Figure S3: TEM images of the nanocrystals obtained by using different surfactants:(a) without any surfactants, (b) 160mg CTAC but without PVP, (c) 100mg PVP but without CTAC.

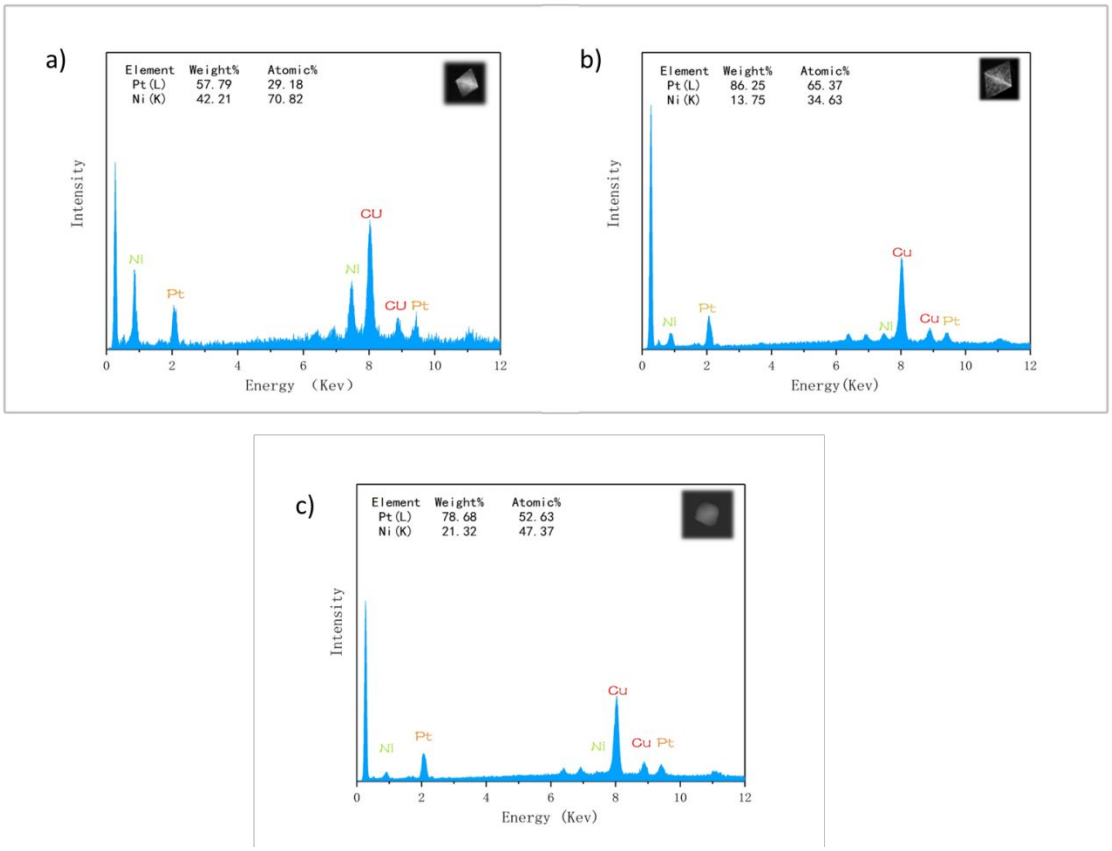

Figure S4: (a) The EDS spectrum of CON. (b) The EDS spectrum of PON. (c) The EDS spectrum of TON.

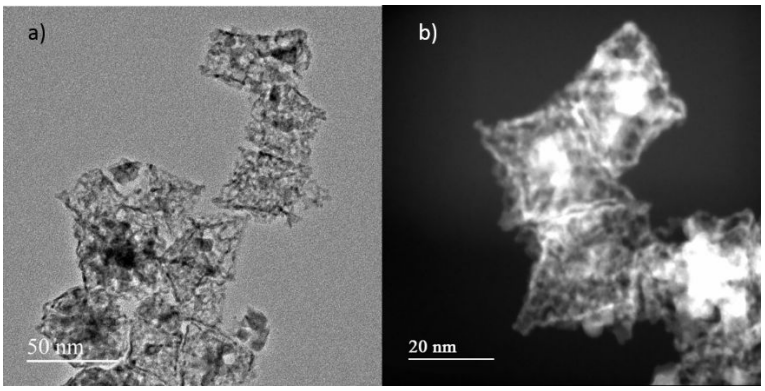

Figure S5: (a) TEM images of the nanocrystals after hydrochloric acid etched (1h, at 100℃). The cores of particles in the center are visible and octahedral structure is warped. (b) STEM image of the nanocrystals after hydrochloric acid etched.

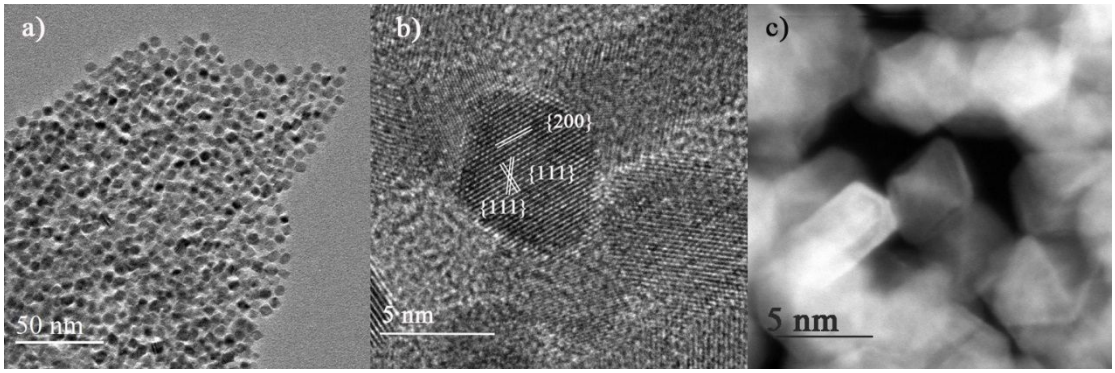

Figure S6: Structure analysis of TON. (a) TEM image of TON. (b) HRTEM image of a TON. (c) STEM image of TON.

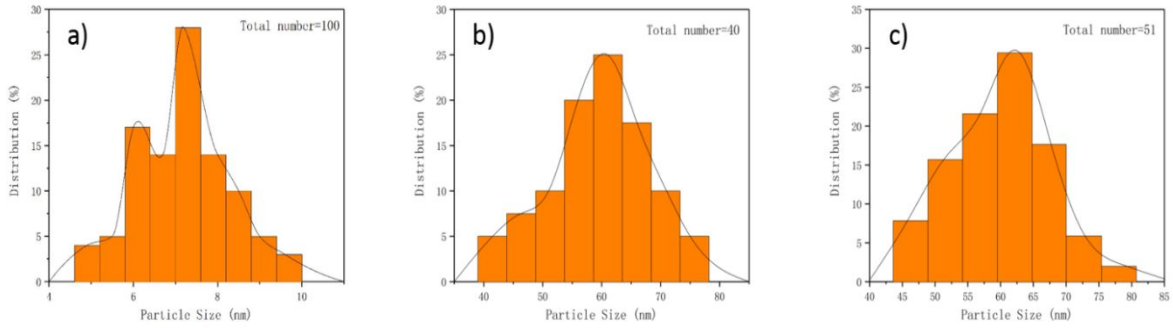

Figure S7: The histograms for particle size distribution. (a) TON, (b) CON, (c) PON.

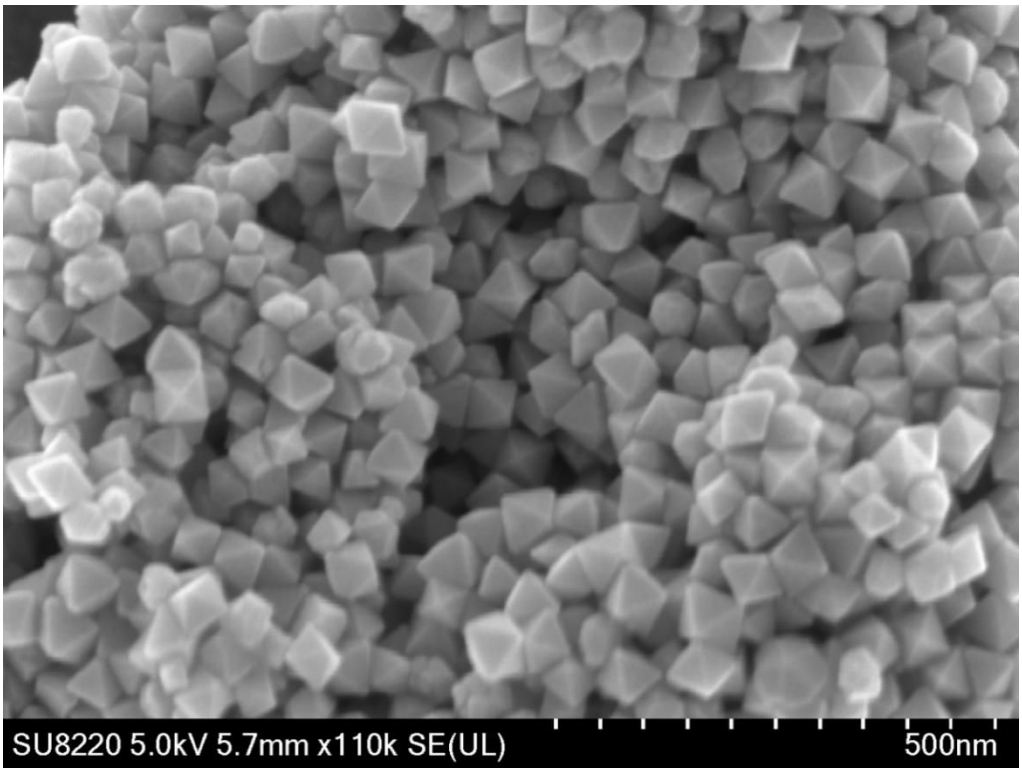

Figure S8: The SEM image of CON.

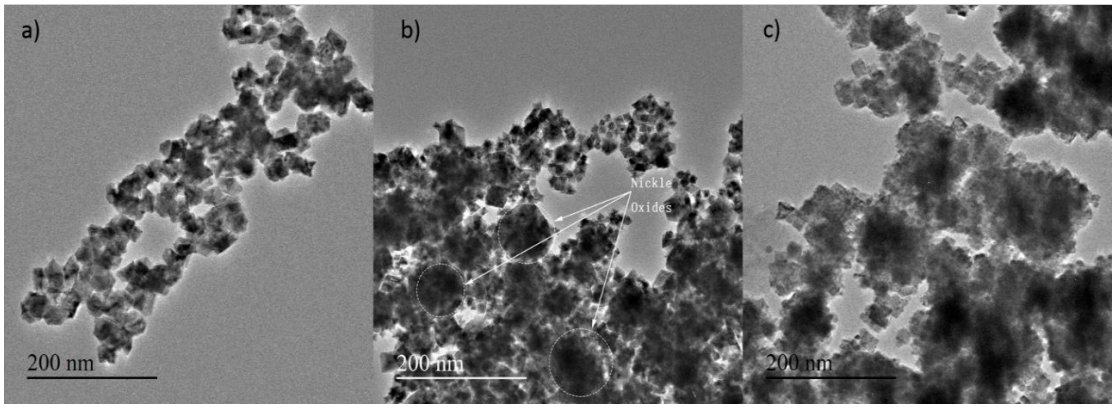

Figure S9: TEM images of the nanocrystals obtained by using different precursors: (a) $Pt(acac)_2$ and $Ni(acac)_2$, (b): H_2PtCl_6(aq) and $Ni(acac)_2$, (c): H_2PtCl_6(aq) and $NiCl_2$. (b) and (c) suggest that water in this synthesis system would lead to the formation of nickle oxides.

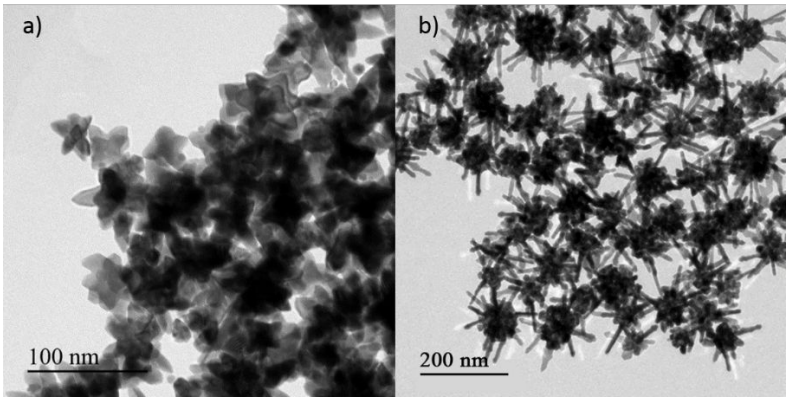

Figure S10: TEM images of the nanocrystals obtained by using different reductant. (a) 10mL Triethylene glycol, (b) 10mL oleylamine.

Table S1: The electrochemical performance and durability of different catalysts for oxygen reduction reaction.

Catalysts	Mass activity ($A\ mg_{Pt}^{-1}$)	Specific activity ($mA\ cm^{-2}$)	ADT (cycles)	ECSA loss ratio (%)	Ref
Pt-Ni nanoframe	0.32	0.55			Ref.14 in text
	0.94	2.8			Ref.15 in text
Pt-Ni nanoparticle	2.1	3.8	4,000	8	Ref.1
		1.09			Ref.2
	0.81	2.13			Ref.3
Pt-Ni porous dendritic nanocrystals	0.757	1.0006	6,000	27.3	Ref.4
	0.93	1.76	1,0000	7	Ref.5
Tiny Pt-Ni octahedral nanoparticle	0.573	1.82	6,000	27.8	This work
Porous and open-structure octahedral Pt-Ni nanoparticle	0.914	2.45	6,000	18.1	This work

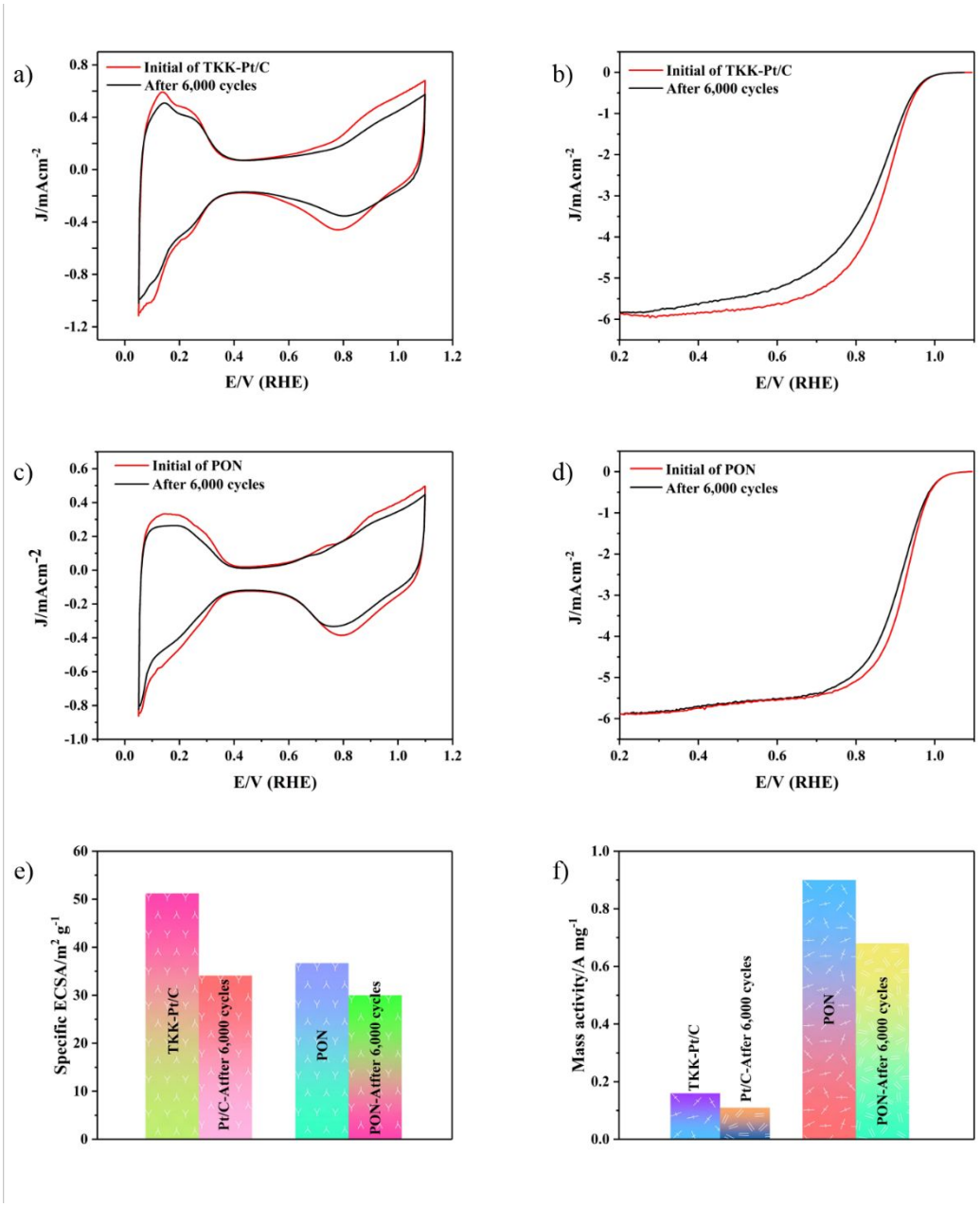

Figure S11: Electrochemical durability of Pt/C catalyst and PON nanocrystals. Cyclic voltammetry (CV) Curves for (a) Pt/C catalyst and (c) PON nanocrystals after prolonged cycles of CV. ORR polarization curves for (b) Pt/C catalyst and (d) PON nanocrystals, initial (black line) and after (red line) 6,000 potential sweep cycles between 0.6 and 1.1 V in an O_2-saturated 0.1 M HClO4 solution at 100 mV/s. (e) and (f) The comparison of ECSA and mass activity of PON and TKK-Pt/C catalyst before and after 6,000 cycles.

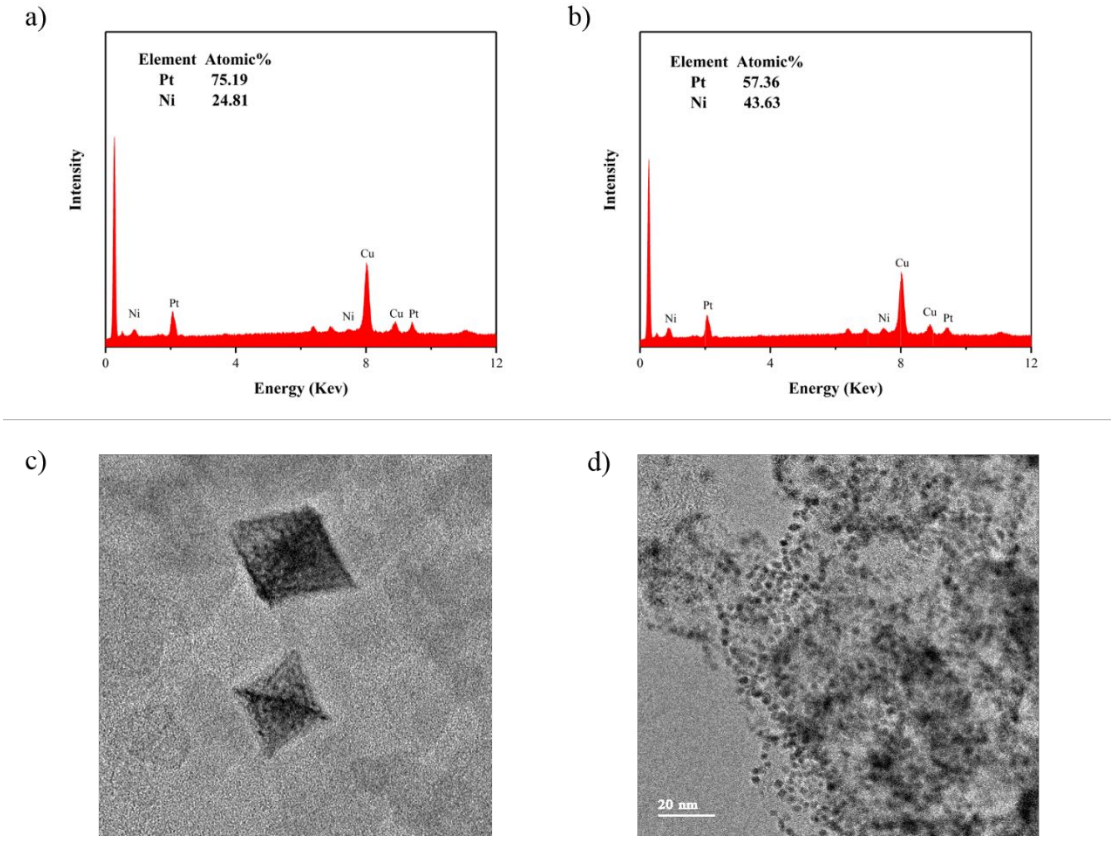

Figure 12: The EDS image of (a) PON, (b) TON after ADT test. The TEM image of (c) PON and (d) TON after ADT test.

Reference:

(1) Changlin, Z.; Youp, H. S.; Alexis, T.; Zhenmeng, P., Solid-state chemistry-enabled scalable production of octahedral Pt-Ni alloy electrocatalyst for oxygen reduction reaction. *Journal of the American Chemical Society* **2014,** *136* , 7805-8.

(2) Xu, X.; Zhang, X.; Sun, H.; Yang, Y.; Dai, X.; Gao, J.; Li, X.; Zhang, P.; Wang, H. H.; Yu, N. F.; Sun, S. G. Synthesis of Pt-Ni alloy nanocrystals with high-index facets and enhanced electrocatalytic properties. *Angew. Chem. Int. Ed. Engl.* **2014,** *53*, 12522-7.

(3) Chang, Q.; Yuan, X. U.; Zhu, S.; Xiao, F.; Shao, M. Pt-Ni nanourchins as electrocatalysts for oxygen reduction reaction. Front. Energy **2017,** *11*, 254-259.

(4) Huang, X.; Zhu, E.; Chen, Y.; Li, Y.; Chiu, C. Y.; Xu, Y.; Lin, Z.; Duan, X.; Huang, Y. A facile strategy to Pt3Ni nanocrystals with highly porous features as an enhanced oxygen reduction reaction catalyst. *Adv. Mater.* **2013,** *25*, 2974-9.

(5) Eid, K.; Wang, H.; Malgras, V.; Alothman, Z. A.; Yamauchi, Y.; Wang, L. Facile Synthesis of Porous Dendritic Bimetallic Platinum–Nickel Nanocrystals as Efficient Catalysts for the Oxygen Reduction Reaction. *Chem. Asian J.* **2016,** *11*, 1388-1393.